Available online at www.sciencedirect.com
SCIENCE DIRECT
Journal of the European Ceramic Society 26 (2006) 2799–2806
www.elsevier.com/locate/jeurceramsoc

Creep in ferroelectrics due to unipolar electrical loading

Q.D. Liu [a], J.E. Huber [b,*]

[a] Department of Engineering, University of Cambridge, Trumpington St, Cambridge CB2 1PZ, UK
[b] Department of Engineering Science, University of Oxford, Parks Rd, Oxford OX1 3PJ, UK

Received 26 February 2005; received in revised form 29 June 2005; accepted 3 July 2005
Available online 22 August 2005

Abstract

Measurements of the time-dependent remanent strain and polarisation due to unipolar electric field loading on initially unpoled, polycrystalline PZT-5H are reported. Specimens were loaded under constant electric field for 300 s, while strain and electric displacement were recorded. Strain gauge drift and electrical leakage in each specimen are corrected using measurements on the same specimen in a fully poled (saturated) state. Linear dielectric and piezoelectric moduli are measured as a function of polarisation in a separate test, allowing remanent strain and polarisation to be deduced from the measured strain and electric displacement data. The hypothesis of a power–law relationship between the remanent polarisation rate and electric field is tested. It is found that a power–law relationship with exponent of about 22 agrees well with the measurements. A relationship governing the saturation of polarisation is given.

Keywords: PZT; Creep; Electrical properties; Time-dependence

1. Introduction

Ferroelectric materials are widely applied as actuators and sensors, exploiting the intrinsic coupling between electro-mechanical, electro-optical, and thermo-electrical properties.[1,2] When loaded with an electric field, ferroelectrics show time-dependent strain and electric displacement behaviour. An understanding of this behaviour is essential for the design of devices such as sensors or actuators subject to DC bias or slowly varying voltages. The design of such devices is aided by models that can predict the strain or electric displacement behaviour given a history of electrical or mechanical loading.

Significant progress has been made in modelling the material response of ferroelectrics and understanding the underlying phenomena in recent years. Rate-independent approaches such as Preisach models,[3,4] micromechanical models [5,6] and phenomenological models [7–10] have been used to describe ferroelectric hysteresis under constant loading rate or over short periods of time. However, where loading rates vary or accuracy over long time periods is needed, rate effects and creep in remanent strain and polarisation should be accounted for.

Linear viscous effects have been included in constitutive models by several researchers.[7,11,12] Chen et al. [13–15] used a relaxation model where the polarisation (represented by the number of aligned dipoles) relaxes towards a steady state dependent on the applied electric field. Power–law creep in the form of viscoplasticity was used by Guillon et al.[16] to describe the evolution of remanent strain and polarisation in response to electric field and stress. They used a high value of power–law exponent to model the response to stress, but a unity value to model the response to an electric field. An alternative modelling approach with power–law creeping behaviour at the microstructural level has also been used [17,18]; here, however, the principal aim in using a power–law formulation was to simplify computation rather than to capture rate effects accurately. A high value of creep exponent was used to approximate rate-independent behaviour. Kim and Jiang [19] used a rate formulation where switching proceeds only when the reduction in Gibbs

* Corresponding author. Tel.: +44 1865 283478; fax: +44 1865 273010.
E-mail address: John.Huber@eng.ox.ac.uk (J.E. Huber).

0955-2219/$ – see front matter © 2005 Elsevier Ltd. All rights reserved.
doi:10.1016/j.jeurceramsoc.2005.07.051

energy (driving force f) exceeds a critical value f_{cr}. The switching rate was then assumed to depend linearly on the difference $f-f_{cr}$. This approach was able to capture the change in ferroelectric hysteresis loops with loading frequency. The question of relating switching transformation rates in a ferroelectric crystal to the applied loading rates remains open, and in need of improved experimental data.

Whilst several researchers have investigated creep behaviour under mechanical compressive loads, relatively few investigations explore the electrical creep behaviour of ferroelectrics. Forrester and Kisi [20] investigated ferroelastic switching in poled and unpoled TRS600 ceramics (soft PZT) subjected to compressive stresses from 10 MPa to 60 MPa. Significant creep was observed at stresses as low as 10 MPa. They found that the creep rate dropped rapidly with time, indicating a saturation process, and was strongly dependent on the applied stress. Their data could be modelled by assuming that strain followed a power–law function of time; however, the fitting parameters needed were individual to each load level and thus did not identify a relationship between stress and creep rate. Guillon et al. [21] conducted similar compressive creep tests on poled and unpoled soft PZT at two different temperatures. They model the observed creep strain rate using a power–law dependence on stress, with kinematic hardening. The resulting viscoplastic phenomenological model captures the observed behaviour qualitatively. Creep strain measurements under a constant electric field, less than the coercive field, were carried out at cryogenic temperatures by Pérez-Enciso et al. [22] They found that creep strains depended logarithmically on time beyond 300 μs.

To the authors' knowledge, direct measurements of creep in remanent strain and remanent polarisation as a function of electrical field loading have not been reported in the literature. The measurement of remanent quantities in creep conditions is complicated by the fact that the dielectric permittivity and piezoelectric coefficients also evolve with time. Guillon et al. [16,21] assumed that the piezoelectric coefficients d_{33} and d_{31} evolve in a linear relationship with remanent polarisation, however, they do not confirm this experimentally.

In the present work, the dependence of creep strain rates and polarisation rates on electric field loading is measured, by applying constant electric field E_3 to unpoled samples of PZT-5H material. Since practical measurements yield only the total strain and electric displacement, the remanent parts of these quantities must be inferred by taking account of piezoelectric and dielectric behaviour. In order to account for the evolution of dielectric and piezoelectric moduli (d_{33}, d_{31} and κ_{33}), their values are measured as a function of remanent polarisation in a separate test. Corrections are also made for strain gauge drift and electrical leakage. The results are used to test the hypothesis of power–law creeping or viscoplastic behaviour, and to find a hardening law which governs the saturation of switching.

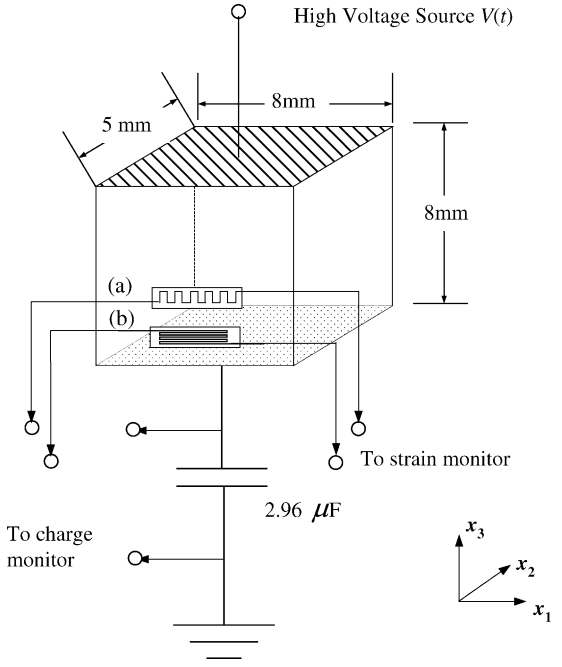

Fig. 1. General arrangement of test equipment for the electrical field-induced creep measurements. Each specimen was immersed in oil when tested: (a) ε_{33} strain gauge measurement and (b) ε_{11} strain gauge measurement.

2. Experimental procedure and results

2.1. Experimental arrangement

Two separate experiments were designed to measure the electrically induced creep behaviour of ferroelectrics. In the first experiment, the total strain and electric displacement were measured as a function of time under a constant electric field. The second experiment employed a series of unipolar square pulses of electric field to increase the polarisation incrementally and to measure the piezoelectric and dielectric coefficients as a function of polarisation. Soft ferroelectric ceramic PZT-5H[1] with a grain size of 5–10 μm and Curie temperature of approximately 195 °C was used in both experiments. Preliminary tests gave the coercive field E_c as 0.7 MV m^{-1}, and the saturation remanent polarisation P_0 as 0.26 C m^{-2}, measured after poling with a field strength of $3E_c$.

Specimens were prepared by dicing unpoled, bulk PZT-5H plates of thickness 5 mm into 8 mm × 8 mm × 5 mm specimens. The applied electric field direction was perpendicular to the surface of the 8 mm × 5 mm faces, each of which was coated with silver-loaded paint to form a conductive electrode (see Fig. 1). Wires were connected onto the electrodes using silver loaded epoxy. A Sawyer–Tower circuit [24] was used to measure electric displacement D_3, and strain gauges were used to measure strain parallel and perpendicular to the

[1] Morgan Matroc Ltd., Vauxhall Industrial Estate, Ruabon, Wrexham, England LL14 6HY, UK.

applied field (ε_{33} and ε_{11}, respectively). The specimen was immersed in an oil bath at room temperature and connected to a high-voltage source (Trek 20/20C amplifier, driven under computer control). Data points were sampled at 500 Hz. A current control was set to limit the maximum polarisation rate achievable in the experiments to 250 C m^{-2} s^{-1}, corresponding to full poling of the sample in 1 ms. A separate check on strain gauge drift was made over a 30 min period, with the drift found to be within 2×10^{-6} min^{-1}.

2.2. Measurement of electric field-induced creep

The aim is to measure the evolution of remanent creep strains $\varepsilon^{\mathrm{r}}_{33}$, $\varepsilon^{\mathrm{r}}_{11}$ and polarisation P^{r}_3 with time t under a constant electric field E_3. Each specimen is initially in an unpoled (isotropic) state. In general the constitutive equation relating the strain and electric displacement (ε_{ij}, D_i) to the applied stress and electric field (σ_{kl}, E_k) of a ferroelectric can be expressed as:

$$\varepsilon_{ij} = S_{ijkl}\sigma_{kl} + d_{kij}E_k + \varepsilon^{\mathrm{r}}_{ij}, \tag{1a}$$

$$D_i = d_{ikl}\sigma_{kl} + \kappa_{ik}E_k + P^{\mathrm{r}}_i \tag{1b}$$

where S_{ijkl}, d_{kij} and κ_{ik} are the elastic compliance, piezoelectric and dielectric tensors. By symmetry, for the present loading, the remanent strain components satisfy $\varepsilon^{\mathrm{r}}_{22} = \varepsilon^{\mathrm{r}}_{11}$ throughout, whilst all shear strain components are zero. Ferroelectric switching processes typically conserve volume and thus it is expected that $\varepsilon^{\mathrm{r}}_{22} = -\varepsilon^{\mathrm{r}}_{33}/2$. Similarly, the remanent polarisation components satisfy $P^{\mathrm{r}}_1 = P^{\mathrm{r}}_2 = 0$. Since the remanent quantities are not readily measured, the strategy is to measure the total strain and electric displacement, and subsequently to find the remanent quantities by subtracting the reversible components. When a saturated state is approached the strain and electric displacement rates $\dot{\varepsilon}_{33}$, $\dot{\varepsilon}_{11}$, and $\dot{D}_3$ approach zero; it thus becomes important to correct for any leakage rate $\dot{D}^{\mathrm{leak}}_3$, or steady strain gauge drift $\dot{\varepsilon}^{\mathrm{err}}_{33}$ and $\dot{\varepsilon}^{\mathrm{err}}_{11}$. Here $\dot{D}^{\mathrm{leak}}_3$ is the apparent rate of electric displacement due to leakage current accumulating at the metering capacitor in the Sawyer–Tower circuit. Likewise $\dot{\varepsilon}^{\mathrm{err}}_{ij}$ is the apparent strain rate due to drift in the metering system. A guard ring system could be used to eliminate $\dot{D}^{\mathrm{leak}}_3$, but has the disadvantage of causing a non-uniform electric field within the specimen. In this work, leakage and strain gauge drift have been measured on each specimen to allow a correction to be made. The loading path $E_3(t)$ shown in Fig. 2 was used to make the direct creep measurements and corrections for each specimen.

Fig. 2 shows an initial dwell period OA followed by a step loading AB with electric field, up to $E_3 = \alpha E_{\mathrm{c}}$. In Fig. 2 the loading corresponds to $\alpha = 1.5$. Tests were conducted at values of α equal to 0.1, 0.3, 0.5, 0.7, 0.9, 1.0, 1.1, 1.3 and 1.5. The constant electric field E_3 in stage BC was held for 300 s to measure the creep strain and remanent polarisation. All subsequent loading was for the purpose of providing information to correct the measurements made during stage BC. Step CD was applied, increasing the electric field E_3 to $3E_{\mathrm{c}}$

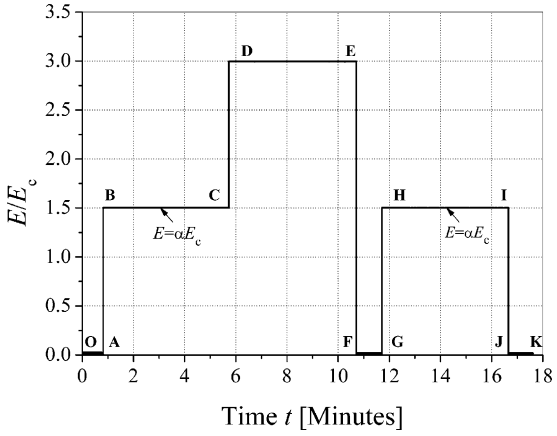

Fig. 2. The electric field loading history applied to a typical specimen. Each of the stages BC, DE and HI has constant electric field held for 5 min.

so that during stage DE of the loading, each specimen was rapidly poled to saturation ($P^{\mathrm{r}}_3 = P_0$), regardless of the prior load level.

With the material fully poled, the electrical loading was removed and a short dwell period FG was used to check that a stable state was reached. Finally, stage HI with $E_3 = \alpha E_{\mathrm{c}}$ was used to measure the steady leakage and strain gauge drift rates $\dot{D}^{\mathrm{leak}}_3$, $\dot{\varepsilon}^{\mathrm{err}}_{33}$ and $\dot{\varepsilon}^{\mathrm{err}}_{11}$. The validity of this measurement is based on the assumption that the material remains fully saturated during stage HI, and thus that the creep rates $\dot{\varepsilon}^{\mathrm{r}}_{33}$, $\dot{\varepsilon}^{\mathrm{r}}_{11}$ and $\dot{P}^{\mathrm{r}}_3$ are zero. The measured electric displacement rate and strain rates then give $\dot{D}^{\mathrm{leak}}_3$, $\dot{\varepsilon}^{\mathrm{err}}_{33}$ and $\dot{\varepsilon}^{\mathrm{err}}_{11}$ directly. In practice, any reversal of switching during the unloading step EF may result in incomplete saturation at the start of stage HI. However, for PZT-5H, the electric displacement response during stage EF was very nearly linear with electric field, suggesting that the extent of switching during unloading was slight. As a further check on the hypothesis that the material remained saturated during stage HI, note that whilst there was significant leakage $\dot{D}_3$ during stage HI, the strain gauge measurements remained almost constant, with drift comparable to that at zero electric field. This is consistent with a scenario where conduction around the specimen was the predominant cause of an apparent $\dot{D}_3$ during stage HI. In order to minimise the influence of any transient from step GH, the steady leakage and drift rates were assessed over the last 240 s of section HI. Note that other electroceramics such as hard PZT can show significant reversal of switching on unloading from the poled state; it would then be preferable to omit stage FG of loading, returning directly from state E to state H.

The measured electric displacement D^{m}_3 (including leakage) and measured strains $\varepsilon^{\mathrm{m}}_{33}$, $\varepsilon^{\mathrm{m}}_{11}$ under uniaxial electrical field loading E_3, with zero stress, can be expressed using Eq. (1) as follows:

$$D^{\mathrm{m}}_3 = D_3 + D^{\mathrm{leak}}_3 = \kappa_{33}E_3 + P^{\mathrm{r}}_3 + D^{\mathrm{leak}}_3, \tag{2a}$$

$$\varepsilon^{\mathrm{m}}_{33} = \varepsilon_{33} + \varepsilon^{\mathrm{err}}_{33} = d_{33}E_3 + \varepsilon^{\mathrm{r}}_{33} + \varepsilon^{\mathrm{err}}_{33}, \tag{2b}$$

$$\varepsilon^{\mathrm{m}}_{11} = \varepsilon_{11} + \varepsilon^{\mathrm{err}}_{11} = d_{31}E_3 + \varepsilon^{\mathrm{r}}_{11} + \varepsilon^{\mathrm{err}}_{11}, \tag{2c}$$

where κ_{33}, d_{33} and d_{31} are dielectric and piezoelectric coefficients. Using steady leakage rates from loading stage HI, the measured quantities in stage BC were corrected to give D_3, ε_{33} and ε_{11}.

In order to construct values of the remanent quantities P_3^r, ε_{33}^r and ε_{11}^r of stage BC, Eq. (2) can be used, noting that κ_{33}, d_{33} and d_{31} evolve with time when holding E_3 constant. It is physically reasonable to assert that the coefficients κ_{33}, d_{33} and d_{31} can be expressed as unique functions of the material state variables P_3^r, ε_{33}^r and ε_{11}^r in this experiment. If additionally, for these uniaxial tests, the remanent strains ε_{33}^r and ε_{11}^r can be expressed as a single valued function of polarisation P_3^r, then (2a) can be rewritten as

$$D_3 = \kappa_{33}(P_3^r)E_3 + P_3^r \tag{3}$$

and P_3^r can be recovered for a given E_3 provided that the function $\kappa_{33}(P_3^r)$ is known. Having recovered P_3^r, provided the corresponding functions $d_{33}(P_3^r)$ and $d_{31}(P_3^r)$ are known, then the remanent strains ε_{33}^r and ε_{11}^r can be found. In Section 2.3, measurements of the dielectric and piezoelectric coefficients are made as functions of polarisation and the accuracy of the assertion that polarisation can be used as a unique state variable for this uniaxial loading is checked.

2.3. Measurement of the state-dependent material parameters κ_{33}, d_{33} and d_{31}

In order to measure κ_{33}, d_{33} and d_{31} as functions of the remanent polarisation P_3^r a fresh material specimen identical to those described in Section 2.2 was prepared, and connected to the test apparatus as shown in Fig. 1. A series of positive square pulses of electric field, of duration 1 s and steadily increasing magnitude, was applied to the specimen while the material response (D_3^m, ε_{33}^m, ε_{11}^m) was measured. The pattern of loading, shown in Fig. 3, was designed to increase the remanent polarisation in small steps, whilst providing a series of electric field jumps ΔE_3 that would allow κ_{33}, d_{33} and d_{31} to be assessed according to:

$$\kappa_{33} = \frac{\Delta D_3}{\Delta E_3}, \tag{4a}$$

$$d_{33} = \frac{\Delta \varepsilon_{33}}{\Delta E_3}, \tag{4b}$$

$$d_{31} = \frac{\Delta \varepsilon_{11}}{\Delta E_3}. \tag{4c}$$

Here $\Delta\varepsilon_{33}$, $\Delta\varepsilon_{11}$ and ΔD_3 are the jumps in strain and electric displacement measured over electric field jump ΔE_3. Each jump ΔE_3 occurred within 4 ms and thus leakage and strain gauge drift can be neglected in Eq. (4a–c). Furthermore, the greatest increment of electric displacement during any pulse in the experiment was 0.0044 C m^{-2} (~1.7% P_0) and thus changes in polarisation P_3^r are also neglected in Eq. (4a–c). Note that a significant error in the calculated κ_{33} is expected at the start of the test, when each jump ΔD_3 or ΔE_3 is small. During each dwell period of 1 s at $E_3 = 0$, the measured electric displacement provided a value of remanent polarisation P_3^r corresponding to the unloading step at the end of the previous pulse, and the loading step at the start of the following pulse in E_3. The experiment was stopped after about 400 s; at this point the jumps in electric field ΔE_3 were of magnitude $1.7E_c$ and the remanent polarisation was close to saturation.

The resulting measurements of $\kappa_{33}(P_3^r)$ are shown (dotted) in Fig. 4. Results corresponding to both the loading and unloading steps are included. Except for a small region ($P_3^r < 0.02$ C m^{-2}) at the start of the test, the measurements agree well with a linear fit of the form:

$$\kappa_{33}(t) = \kappa_{33}(0) + (\kappa_{33}(P_0) - \kappa_{33}(0))\frac{P_3^r}{P_0}, \tag{5}$$

with the saturation polarisation $P_0 = 0.26$ C m^{-2} and the parameters $\kappa_{33}(0) = 2.55 \times 10^{-8}$ F m^{-1}, $\kappa_{33}(P_0) = 4.20 \times 10^{-8}$ F m^{-1}. Here $\kappa_{33}(0)$ corresponds to the dielectric permittivity of the unpoled material, while $\kappa_{33}(P_0)$ is the

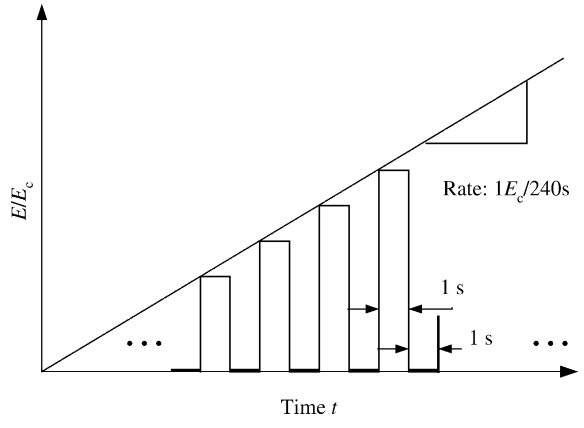

Fig. 3. A series of electrical pulses applied to the PZT-5H specimens to measure the variation of κ_{33}, d_{33} and d_{31} with remanent polarisation.

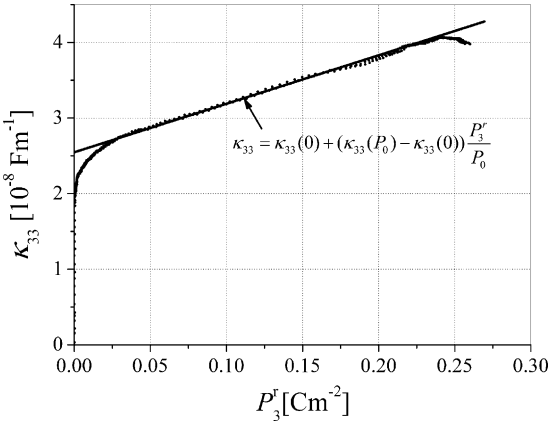

Fig. 4. Dielectric permittivity coefficient κ_{33} as a function of the remanent polarisation P_3^r. Measured points are shown as a dotted curve, and a straight line fit is shown as a solid line.

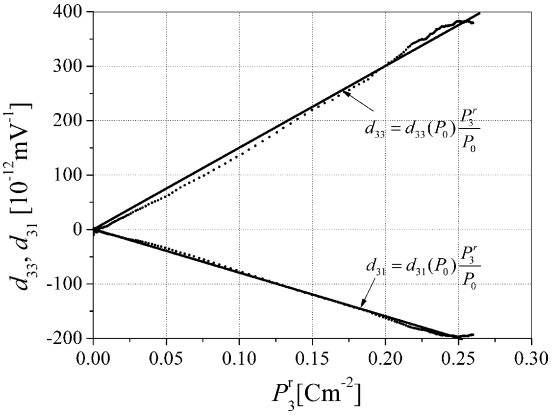

Fig. 5. Piezoelectric coefficients d_{33} and d_{31} as a function of the remanent polarisation P_3^r. Measured points are shown as a dotted curve, and a straight line fit is shown as a solid line.

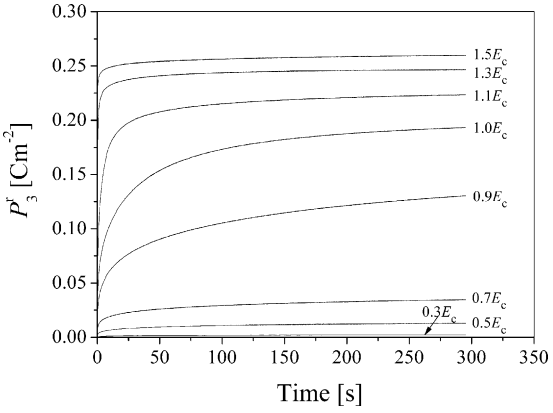

Fig. 6. Measured P_3^r values evolving with time under various magnitudes of constant electric field.

dielectric permittivity of the fully poled material. The linear fit is shown (solid line) in Fig. 4. The corresponding set of measurements of d_{33} and d_{31} are shown in Fig. 5. Here again, a good agreement to a linear fit with polarisation is found as follows:

$$d_{33}(P_3^r) = d_{33}(P_0)\frac{P_3^r}{P_0}, \qquad d_{31}(P_3^r) = d_{31}(P_0)\frac{P_3^r}{P_0} \tag{6}$$

using the parameters $d_{33}(P_0) = 3.80 \times 10^{-10}\,\mathrm{mV}^{-1}$, $d_{31}(P_0) = -2.07 \times 10^{-10}\,\mathrm{mV}^{-1}$. Linear relationships between permittivity or piezoelectric coefficients of this type have been assumed by several authors.[11,13–16]

As a check on the results in Figs. 4 and 5, the measurements of κ_{33}, d_{33} and d_{31} as functions of remanent polarisation were repeated on fresh material specimens, using a different pattern of loading. In these separate tests, a series of electric field pulses of constant magnitude and duration 1 s was applied to each specimen. The test was repeated three times with three distinct step magnitudes: $0.7E_c$, $0.8E_c$ and $0.9E_c$. The results were found to be consistent with Figs. 4 and 5 to within a few percent over 90% of the range of P_3^r. Note that these extra tests were not individually able to capture κ_{33}, d_{33} and d_{31} over the whole range of P_3^r values: the $0.7E_c$ loading never achieved full saturation, whilst the $0.8E_c$ and $0.9E_c$ loading produced large steps in P_3^r at the start of the test.

2.4. Results

By substituting Eq. (5) into Eq. (3) approximate values of $P_3^r(t)$ can be constructed from the corrected electric displacement measurements $D_3(t)$ during section BC of the loading curve shown in Fig. 2. The values of $P_3^r(t)$ are given by

$$P_3^r(t) = P_0\frac{D_3(t) - \kappa_{33}(0)E_3}{P_0 + (\kappa_{33}(P_0) - \kappa_{33}(0))E_3} \tag{7}$$

and plotted in Fig. 6. The results corresponding to $E_3 = 0.1E_c$ are omitted from Fig. 6; at this low level of loading the total creep in remanent polarisation observed was of order $10^{-3}\,\mathrm{C\,m^{-2}}$. Higher field levels in Fig. 6 correspond to a more rapid approach to the saturated state, but it is worth noting that at loading levels close to the coercive field, there is still a significant creep rate 300 s after the loading is first applied. At high or low field levels, relative to E_c, the polarisation response appears flat after a few seconds: at high fields this corresponds to saturation being approached, whilst at low field levels, the creep process is ongoing but slow.

The remanent strains $\varepsilon_{33}^r(t)$ and $\varepsilon_{11}^r(t)$ can be constructed similarly, using Eqs. (2b and c) and (6), employing the calculated values of $P_3^r(t)$. The results are shown in Fig. 7, again with the $E_3 = 0.1E_c$ results omitted for clarity. Similar trends are seen as in Fig. 6, and additionally the results closely follow volume conserving axisymmetric behaviour ($\varepsilon_{11}^r = -\varepsilon_{33}^r/2$).

In constructing the values of $P_3^r(t)$, $\varepsilon_{33}^r(t)$ and $\varepsilon_{11}^r(t)$, the assumption that a single internal state variable, P_3^r, can describe the material state during uniaxial electric field loading has been made. As a check on the validity of this assumption, Fig. 8 shows $\varepsilon_{33}^r(t)$ versus $P_3^r(t)$ for each level of loading; a single line would be expected if the assumption were correct. It appears that the functional dependence of remanent strain on polarisation during uniaxial electric field loading is influenced by the electric field magnitude. However, the results in Fig. 8 follow a

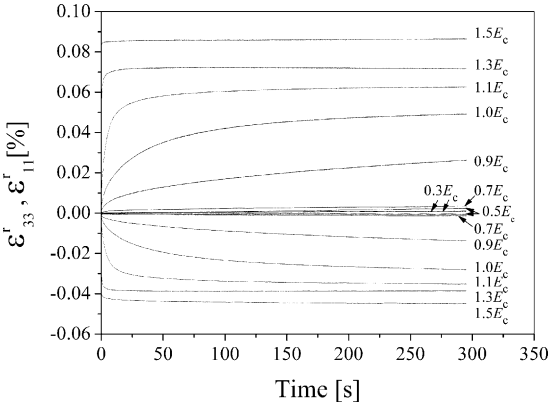

Fig. 7. Measured ε_{33}^r and ε_{11}^r values evolving with time under various magnitudes of constant electric field.

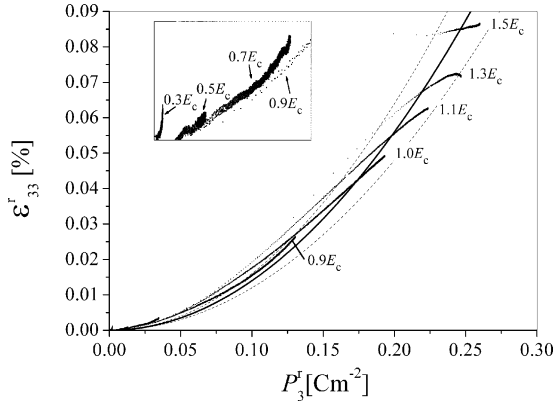

Fig. 8. Remanent strain ε^r_{33} vs. remanent polarisation P^r_3 evolving at several levels of applied electric field loading E_3.

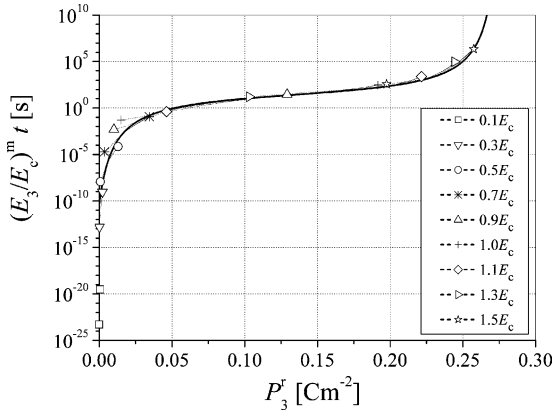

Fig. 9. Measured values of $(E_3/E_c)^m t$ vs. polarisation P^r_3 at various levels of constant electric field E_3. Measured data are shown as dashed lines, with symbols marking the end points of each set of data. The fitting function $f(P^r_3)$ is shown as a solid line.

quadratic strain–polarisation relationship approximately,

$$\frac{\varepsilon^r_{33}}{\varepsilon_0} = \left(\frac{P^r_3}{P_0}\right)^2 \tag{8}$$

with $\varepsilon_0 \sim 0.085\%$. Eq. (8) is shown as a solid line in Fig. 8, whilst dashed lines indicate a $\pm 15\%$ range on ε_0.

3. Modelling of electrical field-induced creep

Steady creep in metals and other materials is often modelled by a power–law relationship between strain rate and stress at temperatures above one-third of the absolute melting point T_m. Whilst tests at room temperature on electroceramics are conducted at well below $T_m/3$, the Curie temperature T_c of PZT-5H is about 195 °C and the test temperature was close to $2/3T_c$, so creeping motion of domain walls is expected. Several authors have modelled ferroelectric switching at a microstructural level using a power–law relationship between the switching rate and a driving force, such as the reduction in Gibbs free energy of the system.[17,18] Hutchinson [23] related creep at the microstructural level to the macroscopic creeping behaviour of polycrystals and showed that the macroscopic steady creep exponent is identical to that of individual slip systems. However, in the present study, unsteady creep occurs because of the saturation of the switching process.

To model the uniaxial creep of a ferroelectric under purely electric field loading, a macroscopic power–law creep relationship of the form

$$\frac{\dot{P}^r_3}{\dot{P}_0} = \left(\frac{E_3}{E_c}\right)^m h\left(P^r_3\right) \tag{9}$$

can be postulated, where $\dot{P}_0$ is a rate constant, m is the creep exponent and $h\left(P^r_3\right)$ is a saturation (or hardening) function, with the properties $h(0)=1$ and $h\left(P^r_3\right) \to 0$ as $P^r_3 \to P_s$. Here, P_s is a remanent polarisation limit, representing a fully saturated state. The value of P_s is greater than the remanent polarisation P_0 measured after poling with an electric field of $3E_c$. Defining $h\left(P^r_3\right)$ in this way sets $\dot{P}_0$ as the initial remanent polarisation creep rate for unpoled material loaded at the coercive field. This separable form can be integrated to give

$$f(P^r_3) = \int \frac{dP^r_3}{\dot{P}_0 h\left(P^r_3\right)} = \left(\frac{E_3}{E_c}\right)^m t \tag{10}$$

defining a single valued function $f(P^r_3)$. To demonstrate the validity of Eq. (9), $f(P^r_3)$ is plotted in Fig. 9, using a power–law exponent of $m=22$, which was found to collapse the experimental data to a single line. Since the applied electric field varied over more than an order of magnitude in these tests, the appearance of the data in Fig. 9 is sensitive to the chosen value of m. The fit at $m=22$ is good across a wide range of data, whilst the fit deteriorates severely for $m>23$ or $m<21$. Also shown in Fig. 9 is a curve fit to the experimental data which has the form

$$f(P^r_3) = t_0\, e^{g(P^r_3)} \tag{11}$$

where

$$g(P^r_3) = \left(\frac{P_s}{P_s - \left|P^r_3\right|} - \frac{P_s}{\left|P^r_3\right| + P^*}\right) \tag{12}$$

with $t_0 = 27$ s and $P_s = 0.28\,C\,m^{-2}$. A small offset polarisation $P^* = 0.01\,C\,m^{-2}$ has been introduced into Eq. (12); the fit of the measured data to Eq. (12) is insensitive to the value of P^* in the range $0 < P^* < 0.01\,C\,m^{-2}$, however, a non-zero value of P^* avoids singularity of $g(P^r_3)$ at $P^r_3 = 0$. The physical meaning of t_0 is the time taken, under loading with the coercive field $E=E_c$, for the polarisation magnitude to reach $(P_s - P^*)/2$. The three constants t_0, P_s and P^* fix the initial polarisation rate $\dot{P}_0$ under loading with $E=E_c$ at $\dot{P}_0 = 7.0 \times 10^6 C\,m^{-2}$. The value of $\dot{P}_0$ is very sensitive to P^*: in the experiments, the initial polarisation rates were very high and were not measured accurately. For this reason, it is preferable to define the model in terms of the physically meaningful quantities t_0, and P_s, rearranging Eqs. (9), (11)

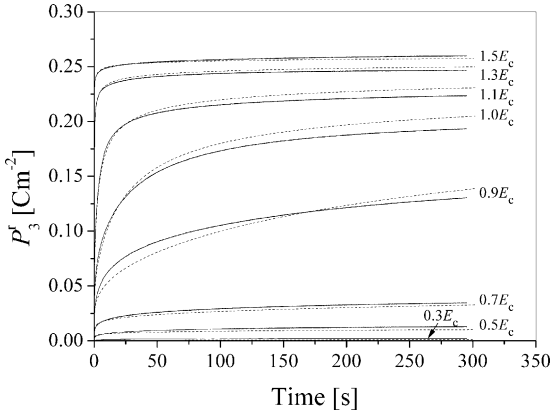

Fig. 10. Measured and modelled P_3^r values evolving with time under various magnitudes of constant electric field. Measured data are shown as solid lines and the power–law creeping model is shown as dashed lines.

and (12) to give the polarisation rate $\dot{P}_3^r$ as

$$\dot{P}_3^r = \left(\frac{E_3}{E_c}\right)^m \frac{e^{-g(P_3^r)}}{t_0 g'(P_3^r)} \tag{13}$$

where differentiation is indicated with a dash.

Using Eqs. (12) and (13), the material response to constant electric field at each loading level of Fig. 6 can be calculated. The model response is shown (dashed) in Fig. 10, and the experimental data is reproduced, for comparison, using solid lines. The proposed saturation function $h(P_3^r)$ provides a good fit to the measured data. Note, however, that this form of saturation function is suitable only for unipolar (forward) loading with electric field. Under fully reversed (cyclic) loading, stable hysteresis loops are in practice obtained, suggesting a kinematic hardening mechanism, or a softening behaviour. Further measurements are needed to identify an appropriate functional description of this behaviour. In particular, measurement of remanent strain and polarisation rates under reversed loading from the poled state are needed.

4. Conclusions

Creep of the remanent strain and polarisation in ferroelectric ceramic PZT-5H has been measured at constant electric field, starting from an unpoled state. The tests revealed that the evolution of remanent strain and polarisation with time depends on both the electric field magnitude and the state of the material, which was characterised here by its remanent polarisation. At electric field values less than the coercive field, slow but stable creep was observed, whereas above the coercive field, rapid switching was followed by gradual saturation. The remanent polarisation rate was found to fit a power–law relationship with applied electric field, controlled by a saturation factor which is a function of remanent polarisation only. A power–law exponent of 22 gave a good fit to the measured data. This high value of exponent is suggestive of nearly rate-independent behaviour; however, saturation effects reduce the strain and polarisation rates, resulting in a very gradual approach towards the fully saturated state, even at high electric field values. The data suggest that caution is needed in applying rate-independent models of ferroelectric switching when the field levels are of the order of the coercive field or less, and this motivates further development of rate-dependent approaches. Whilst the data presented here were measured on a single material composition, similar behaviour was also observed in other polycrystalline compositions and in single crystals; that work will be published in a separate study. In order to measure the remanent strain and polarisation it was necessary to account for the evolution of dielectric and piezoelectric behaviour with time. The dielectric and piezoelectric coefficients were found to vary nearly linearly with remanent polarisation during poling. Further investigation is needed to characterise creep under reversed loading or in the presence of combined mechanical and electrical loading.

Acknowledgements

This work forms part of the research programme of the Netherlands Institute for Metals Research (NIMR) and the Stichting voor Fundamenteel Onderzoek der Materie (FOM).

References

1. Nye, J. F., *Physical Properties of Crystals: Their Presentation by Tensors and Matrices*. Oxford Science Publications, Oxford, 1985.
2. Cao, H. and Evans, A. G., Nonlinear deformation of ferroelectric ceramics. *J. Am. Ceram. Soc.*, 1993, **76**, 890–896.
3. Robert, G., Damjanovic, D. and Setter, N., Preisach modeling of piezoelectric nonlinearity in ferroelectric ceramics. *J. Appl. Phys.*, 2001, **89**, 5067–5074.
4. Cima, L. and Laboure, E., A model of ferroelectric behavior based on a complete switching density. *J. Appl. Phys.*, 2004, **95**, 2654–2659.
5. Hwang, S. C., Lynch, C. S. and McMeeking, R. M., Ferroelectric/ferroelastic interactions and a polarization switching model. *Acta Metall. Mater.*, 1995, **43**, 2073–2084.
6. Huber, J. E., Fleck, N. A., Landis, C. M. and McMeeking, R. M., A constitutive model for ferroelectric polycrystals. *J. Mech. Phys. Solids*, 1999, **47**, 1663–1697.
7. Bassiouny, E., Ghaleb, A. F. and Maugin, G. A., Thermodynamical formulation for coupled electromechanical hysteresis effects. Part I. Basic equations, and Part II. Poling of ceramics. *Int. J. Engng. Sci.*, 1988, **26**, 1279–1306.
8. Cocks, A. C. F. and McMeeking, R. M., A phenomenological constitutive law for the behavior of ferroelectric ceramics. *Ferroelectrics*, 1999, **228**, 219–228.
9. Kamlah, M. and Tsakmakis, C., Phenomenological modeling of the non-linear electromechanical coupling in ferroelectrics. *Int. J. Solids Struct.*, 1999, **36**, 669–695.
10. Landis, C. M., Fully coupled, multi-axial, symmetric constitutive laws for polycrystalline ferroelectric ceramics. *J. Mech. Phys. Solids*, 2002, **50**, 127–152.
11. Kamlah, M. and Jiang, Q., A constitutive model for ferroelectric PZT ceramics under uniaxial loading. *Smart Mater. Struct.*, 1999, **8**, 441–459.
12. Yoo, I. K. and Desu, S. B., Modeling of the hysteresis of ferroelectric thin-films. *Philos. Mag. B*, 1994, **69**, 461–469.

13. Chen, P. J. and Peercy, P. S., One-dimentional dynamic electromechanical consititutive relations of ferroelectric material. *Acta Mech.*, 1979, **31**, 231–241.
14. Chen, P. J. and Madsen, M. M., One dimensional polar responses of the electrooptic ceramic PLZT 7/65/35 due to domain switching. *Acta Mech.*, 1981, **41**, 255–264.
15. Chen, P. J. and Tucker, T. J., One dimensional polar mechanical and dielectric responses of the ferroelectric ceramic PZT 65/35 due to domain switching. *Int. J. Engng. Sci.*, 1981, **19**, 147–158.
16. Guillon, O., Thiebaud, F., Delobelle, P. and Perreux, D., Modelling of the electromechanical behaviour of PZT. *J. Phys. IV France*, 2004, **115**, 85–92.
17. Huber, J. E. and Fleck, N. A., Multi-axial electrical switching of a ferroelectric: theory versus experiment. *J. Mech. Phys. Solids*, 2001, **49**, 785–811.
18. Kamlah, M., Liskowsky, A. C., McMeeking, R. M. and Balke, H., Finite element simulation of a polycrystalline ferroelectric based on a multidomain single crystal switching model. *Int. J. Solids Struct.*, 2005, **42**, 2949–2964.
19. Kim, S. J. and Jiang, Q., A finite element model for rate-dependent behavior of ferroelectric ceramics. *Int. J. Solids Struct.*, 2002, **39**, 1015–1030.
20. Forrester, J. S. and Kisi, E. H., Ferroelastic switching in a soft lead zirconate titanate. *J. Europ. Ceram. Soc.*, 2004, **24**, 595–602.
21. Guillon, O., Thiébaud, F., Deleobelle, P. and Perreux, D., Compressive creep of PZT ceramics: experiments and modelling. *J. Europ. Ceram. Soc.*, 2004, **24**, 2547–2552.
22. Pérez-Enciso, E., Agrait, N. and Vieira, S., Experimental evidence of nonactivated creep in Pb(ZrxTi1-x)O-3 ceramics at low temperatures. *Phys. Rev. B*, 1997, **56**, 2900–2903.
23. Hutchinson, J. W., Bounds and self-consistent estimates for creep of polycrystalline materials. *Proc. R. Soc. Lond. A*, 1976, **348**, 101–127.
24. *IEEE Standard Definitions of Primary Ferroelectric Terms*. ANSI/IEEE Std 180-1986. The Institute of Electrical and Electronics Engineers Inc., USA.